ACS APPLIED MATERIALS & INTERFACES

UAEU Libraries Deanship

Subscriber access provided by United Arab Emirates University | Libraries Deanship

Article

Silver nanoclusters for high-efficiency quenching of CdS nanocrystals electrochemiluminescence and sensitive detection of microRNA

Yan-Yan Zhang, Qiu-Mei Feng, Jing-Juan Xu, and Hong-Yuan Chen

ACS Appl. Mater. Interfaces, **Just Accepted Manuscript** • DOI: 10.1021/acsami.5b09129 • Publication Date (Web): 11 Nov 2015

Downloaded from http://pubs.acs.org on November 14, 2015

Just Accepted

"Just Accepted" manuscripts have been peer-reviewed and accepted for publication. They are posted online prior to technical editing, formatting for publication and author proofing. The American Chemical Society provides "Just Accepted" as a free service to the research community to expedite the dissemination of scientific material as soon as possible after acceptance. "Just Accepted" manuscripts appear in full in PDF format accompanied by an HTML abstract. "Just Accepted" manuscripts have been fully peer reviewed, but should not be considered the official version of record. They are accessible to all readers and citable by the Digital Object Identifier (DOI®). "Just Accepted" is an optional service offered to authors. Therefore, the "Just Accepted" Web site may not include all articles that will be published in the journal. After a manuscript is technically edited and formatted, it will be removed from the "Just Accepted" Web site and published as an ASAP article. Note that technical editing may introduce minor changes to the manuscript text and/or graphics which could affect content, and all legal disclaimers and ethical guidelines that apply to the journal pertain. ACS cannot be held responsible for errors or consequences arising from the use of information contained in these "Just Accepted" manuscripts.

ACS Publications

ACS Applied Materials & Interfaces is published by the American Chemical Society.
1155 Sixteenth Street N.W., Washington, DC 20036
Published by American Chemical Society. Copyright © American Chemical Society.
However, no copyright claim is made to original U.S. Government works, or works produced by employees of any Commonwealth realm Crown government in the course of their duties.

Silver nanoclusters for high-efficiency quenching of CdS nanocrystals electrochemiluminescence and sensitive detection of microRNA

Yan-Yan Zhang[1], Qiu-Mei Feng[1], Jing-Juan Xu[*] and Hong-Yuan Chen

State Key Laboratory of Analytical Chemistry for Life Science and Collaborative Innovation Center of Chemistry for Life Sciences, School of Chemistry and Chemical Engineering, Nanjing University, Nanjing 210023, China.

[*] To whom correspondence should be addressed. Tel: +86-25-89687294.

Email: xujj@nju.edu.cn (J.J. Xu)

ABSTRACT:

In this work, oligonucleotide encapusulated silver nanoclusters were applied in the electrochemiluminescence (ECL) system of CdS nanocrystals (NCs)/ $K_2S_2O_8$ based on dual ECL quenching effects. We found that the ECL emission of CdS NCs matched well with the absorption band of oligonucleotide encapsulated Ag nanoclusters, which could act as the energy acceptor of CdS NCs ECL so as to lead to an effective ECL resonance energy transfer (RET). On the other hand, the Ag nanoclusters could also catalyze electrochemical reduction of $K_2S_2O_8$, resulting in increased consumption of ECL coreactant near the working electrode and decreased ECL intensity from CdS NCs. Based on the dual ECL quenching effects, a sensitive ECL biosensor for detection of microRNA was successfully achieved with a wide linear range from 10 fM to 100 pM.

KEY WORDS:

electrochemiluminescence, silver nanoclusters, synergistic quenching effect, resonance energy transfer, microRNA detection

INTRODUCTION

Electrogenerated chemiluminescence (ECL), or chemiluminescence triggered by electrochemical processes, has emerged as a powerful analytical technique because of its unique advantages, such as high sensitivity, low background signal and no need of any external light source.[1-2] It has attracted explosive interests in various bioanalytical applications. Currently one of the main driving forces in this field is to develop efficient strategies for biosensing.[3]

Since the discovery of ECL resonance energy transfer (RET) between CdS:Mn nanocrystals (NCs) and Au nanoparticles (NPs) within short distances in 2009,[4] the ECL quenching effect based on RET has been demonstrated as an effective approach for improvement of biosensing. Some analytical systems based on ECL RET have been explored, such as CdS:Mn NCs-activated CdTe NCs,[5] CdS NCs-$Ru(bpy)_3^{2+}$,[6] RuSi@$Ru(bpy)_3^{2+}$-Au@Ag_2S NPs,[7] graphene quantum dots (GQDs)-Au NPs,[8] and CdTe NCs-Au nanoclusters[9] donor-acceptor pairs. As an effect of energy transfer, distance-dependent plasmon coupling could be applied for enhancement of ECL.[10-11] In addition, ECL biosensors could also be fabricated based on other approaches, such as generation or depletion of coreactants by catalysts,[12-13] modulation of the communication between the electrode and coreactants by impedance effect of proteins or cells,[14-15] and promotion of electron transfer by compositing nanomaterials with ECL emitters.[13, 16]

Previously, our group has enunciated the synergistic effect between electron and energy transfer in an ECL system involving CdS NCs and Au NPs.[17] Upon introduction of TATA-binding protein, ECL RET could happen while the dsDNA was cut off, which remarkably

suppressed the ECL signals due to the curved double stranded DNA structure (dsDNA). Recently, a double-quenched GQDs ECL for quantification of protein kinase A activity was also reported with the confluence effect of reduction of coreactant H_2O_2 resulting from G-quadruplex-hemin DNA enzyme catalytic reaction and ECL RET between Au NPs and GQDs.[8] However, it is still rare to develop sensitive sensing strategies by integrating electron and energy transferring into an ECL platform based on dual enhancing or quenching effects.

It is known that the basic requirements of efficient ECL RET are the spectral overlap between the donor's ECL spectrum and the acceptor's absorption spectrum and their space proximity.[3-4] For example, CdS NCs have been applied as a kind of common ECL emitters with their broad ECL emission peaked at ca. 500 nm.[4] Recently, it has been reported that Ag nanoclusters showed an absorption band at the peak of 492 nm in the UV-vis spectrum by employing specific functional single stranded oligonucleotide sequence as the template and $NaBH_4$ as the reducing agent for reduction of Ag cations.[18] Such Ag clusters might be a good candidate as the energy acceptor of CdS NCs. Moreover, such nanoclusters typically consist of several to tens of atoms with their sizes below 2 nm and have size-dependent discrete energy levels, which probably leads to "molecular" properties such as catalytic activity.[19] Principally, it is possible to incorporate Ag nanoclusters for developing the ECL sensing systems based on the synergistic effect of ECL RET and electron transfer.

MicroRNA (MiRNA) is a class of single-stranded, endogenous, non-protein-coding RNAs with a typical length of 19-23 nucleotides.[20] MiRNA plays significant roles in

post-transcriptional regulation in diverse animals and plants[21-22] and its expression profiling could be used as potential molecular biomarkers for diagnosis.[20, 23-26]

Based on our previous work,[18] herein oligonucleotide encapsulated Ag nanoclusters were applied as the transducers of biological binding events benefited from their potential catalytic ability and overlapped absorption spectrum with the ECL emission of CdS NCs. Our results demonstrated that Ag nanoclusters could not only quench the ECL emissions from CdS NCs by ECL RET, but also catalyze the electro-reduction reaction of $K_2S_2O_8$, making ECL coreactant greatly consumed near the electrode surface and thus leading to an obvious decrease in ECL intensity. We successfully established a quenched ECL sensing system for detection of MiRNA based on the synergistic effect of ECL RET and electron transfer by Ag nanoclusters.

EXPERIMENTAL SECTION

Reagents

Sodium sulfide ($Na_2S·9H_2O$) and potassium peroxydisulfate ($K_2S_2O_8$) were purchased from Nanjing Chemical Co. Ltd. Cadmium nitrate tetrahydrate ($Cd(NO_3)_2·4H_2O$) was supplied by Sinopharm Chemical Reagent Co. Ltd. Tris (2-carboxyethyl) phosphine hydrochloride (TCEP), MCH and sodium borohydride ($NaBH_4$) were obtained from Sigma-Aldrich (St. Louis, MO). Silver nitrate ($AgNO_3$) was bought from Chinasun Specialty Products Co., Ltd. Phosphate buffer solution (0.1 M KH_2PO_4-Na_2HPO_4; PBS; pH 8.3) containing 0.05 M $K_2S_2O_8$ as a coreactant was used for ECL measurements. All other reagents were of analytic grade and used as received. Millipore ultrapure water (resistivity ≥ 18.2 MΩ.cm) was used throughout the experiments. The

oligonucleotides with the following sequences were purchased from Shanghai Sangon Biological Engineering Technology & Services Co., Ltd. (China) and purified using high-performance liquid chromatography. Their sequences were listed as follows:

Molecular beacon (MB):

5'SH-TTT TTT TTT TTT ACT GTC TTA GCA CGC CAA TAT TTA CGT GCT GCT AA-3'

Functional oligonucleotide probe:

5'-TGC TAA GAC AGT ***CCC TAA CTC CCC***-3'

The underlined region of MB represents the stem sequence, and the italic bold letters identify the sequence used for Ag nanoclusters nucleation.

All the RNA sequences were purchased from Nanjing GenScript Co., Ltd. (Nanjing, China) and purified using high-performance liquid chromatography, which were listed as follows:

Target RNA: 5'-UAG CAG CAC GUA AAU AUU GGC G-3'

One base mismatched RNA:

5'-UAG CAG CAC GUA AAU AUU GCC G-3'

Three bases mismatched RNA:

5'-UAA CAG CAC GAA AAU AUU GCC G-3'

The mismatched bases are highlighted in the boxes.

Apparatus

The electrochemical and ECL emission measurements were simultaneously conducted on a MPI-A multifunctional electrochemical and chemiluminescent analytical system (Xi'an Remax Electronic Science & Technology Co. Ltd., Xi'an, China) at room temperature. The biased potential of photomultiplier tube was set at -500 V during detection. The scan rate was 100 mV s^{-1}. The experiments were carried out by using a traditional three-electrode system. A 3 mm diameter glass carbon electrode (GCE) modified with CdS nanocrystals (NCs) film served as the working electrode. Meanwhile, a Pt wire and a silver/silver chloride electrode (SCE) were used as the counter and reference electrodes, respectively. ECL spectra were obtained by a series of optical filters (420, 440, 460, 480, 500, 520, 540, 560, 580, 600, 620, 640, 660 nm). Transmission electron microscopy (TEM) was performed with a JEOL model 2000 instrument operating at 200 kV accelerating voltage. The UV-vis absorption spectra were achieved on a Shimadzu UV-3600 UV-vis-NIR spectrophotometer (Shimadzu Co.). Electron paramagnetic resonance (EPR) experiments were measured on a Bruker spectrometer (EMX-10/12, Bruker, Germany) at room temperature with 5, 5-dimethyl-1-pyrroline N-oxide (DMPO) as a spin-trapping agent. Gel electrophoresis was performed on a DYCP-31 BN electrophoresis analyzer (Liuyi Instrument Company, China) and imaged on the Bio-Rad ChemDoc XRS (USA).

Synthesis of CdS NCs

CdS NCs were prepared according to the previous work in our group with a slight modification.[4] Briefly, after $Cd(NO_3)_2 \cdot 4H_2O$ (0.1861 g) was dissolved in 30 mL ultrapure water and heated up to 70ºC under stirring, a fresh solution of $Na_2S \cdot 9H_2O$ (0.5960 g) in 30 mL

ultrapure water was slowly injected to the above solution, forming a mixture with a Cd^{2+}/ S^{2-} molar ratio of 1: 4, and orange-yellow precipitates were obtained immediately. The reaction temperature was kept constant at 70ºC for 3 h with continuous refluxing. The final reaction solution was centrifuged to collect precipitates, which were washed thoroughly with absolute ethanol and then ultrapure water for two times, respectively. After that, the obtained precipitates were ultrasonically dispersed into ultrapure water for further centrifugation at 9000 rpm for 10 min to collect the upper yellow CdS NCs dispersion, which was then stored at 4 °C for further use.

Preparation of CdS NCs Modified GCE

Firstly, GCE was polished on SiC papers with successively finer grades and then with 0.3 μm alumina powder to make the electrode surface mirror-like. After that, GCE was thoroughly rinsed with water and then sonicated in ultrapure water. By dropping 10 μL of the CdS NCs dispersion onto the pretreated surface of GCE and letting it evaporated in air at room temperature for 16h, CdS NCs/GCE was fabricated. Owning to numerous active sites on the fresh surface of the pretreated GCE, NCs film could be adsorbed on it firmly without any swelling or peeling off after being stored in 20 mM PBS buffer (pH 7.4) solution for one month before use or being further immersed in solution for several hours' modification.

Synthesis of Ag Nanoclusters

Ag nanoclusters were synthesized according to the previous literature.[18] Briefly, 1.44 μL of 25mM $AgNO_3$ solution was added to 450 μL of 10^{-5} M template strand (prepared in 20 mM PBS

buffer containing 1.0 mM Mg^{2+}, pH 7.4) with a Ag^{+}/oligonucleotide relative concentration ratio of 8:1. The mixed solution was vigorously shaken for 1 min and kept in darkness at 4°C for 30 min. Then, 1.44 μL of 12.5 mM freshly prepared $NaBH_4$ solution was added to the above solution under ice temperature and the resulting solution was vigorously shaken for 1 min. The oligonucleotide encapsulated Ag nanoclusters were obtained by keeping the solution overnight in darkness at 4 °C.

Fabrication of MiRNA Biosensor

Firstly, 1 mL of 20 mM PBS buffer (pH 7.4) containing 0.2 μM stem-loop structure probe was activated by 2 μL of 10 mM TCEP at 4 °C for 1 h to cut S-S bonds. The CdS NCs/GCE was immersed in 100 μL of the pretreated DNA solution and incubated overnight at 4 °C to immobilize the probe on the electrode surface. Subsequently, the electrode was rinsed with 20 mM PBS buffer (pH 7.4). After that, the resulting molecular beacon modified electrode (MB/CdS NCs/GCE) was submerged in 60 μL of 20 mM PBS buffer (pH 7.4) containing 100 μM MCH for 1 h to block the surface and force the modified DNA probe to adopt an upright surface orientation that favors further hybridization. Finally, the surface of the electrode (MCH/MB/CdS NCs/GCE) was rinsed with 20 mM PBS buffer (pH 7.4) to remove the nonspecifically adsorbed substance. Thus unlike some other ECL methods in aqueous system or fluorescent detecting technique, here microRNA was detected in a heterogeneous system using MCH/MB/CdS NCs/GCE as a solid-state ECL probe which could reduce the potential interferences of sample matrix.

ECL Measurements

The MCH/MB/CdS NCs/GCE was immerged in 100 μL of 20 mM PBS buffer (pH 7.4) containing 1.0 mM Mg^{2+}, miRNA at different concentrations and 0.2 μM oligonucleotide encapsulated Ag nanoclusters at 37 °C for 60 min. The obtained electrode was rinsed with 20 mM PBS buffer containing 1.0 mM Mg^{2+} (pH 7.4) thoroughly. After each immobilization step, ECL emission signals were measured in 5 mL of 0.1 M PBS (pH 8.3) containing 0.05 M $K_2S_2O_8$ as a coreactant with a scan range from 0 to -1.25 V.

Polyacrylamide Hydrogel Electrophoresis

Different DNA/RNA structures (molecular beacon, target miRNA, functional oligonucleotide probe, molecular beacon after incubation with target miRNA, molecular beacon after incubation with functional oligonucleotide probe, molecular beacon after incubation with the mixture solution of target miRNA and functional oligonucleotide probe) were incubated at 37 °C for 60 min. The obtained DNA/RNA structures were injected into polyacrylamide hydrogel in tris-borate-EDTA (TBE) buffer and electrophoresis was carried out at 100 V for 1 h in TBE buffer. Finally, the obtained board was observed under UV irradiation.

RESULTS AND DISCUSSION

Characterization

As shown in Figure S1A, the TEM image of CdS NCs indicated that the average size of the synthesized CdS NCs was 6.36 ± 0.27 nm. On the other hand, the diameter of CdS NCs was estimated to be 6.23 nm according to the empirical equation[27] and the UV-vis spectrum with an

absorption band edge at 471 nm (Figure S1B, curve a). In the following, CdS NCs with the volume of 10 μL were drop-casted onto the surface of a GCE and used as ECL emitters. As the electrode potential is negative enough, theoretically, CdS NC and $S_2O_8^{2-}$ (the coreactant) could be reduced to be $(CdS)^{\bullet-}$ and $SO_4^{\bullet-}$ radicals, respectively. The anion sulfate radical $SO_4^{\bullet-}$ could lead $(CdS)^{\bullet-}$ into its excited state $(CdS)^*$, which could emit light (ECL signals) in the aqueous solution. As shown in Figure S1B, the ECL emission spectrum of CdS NCs film exhibited a broad emission spectral band with its main peak at ca. 520 nm. The ECL processes above could be described as follows:[28]

$$CdS + ne^- \rightarrow n(CdS)^{\bullet-} \quad (1)$$

$$S_2O_8^{2-} + e^- \rightarrow SO_4^{2-} + SO_4^{\bullet-} \quad (2)$$

$$(CdS)^{\bullet-} + SO_4^{\bullet-} \rightarrow (CdS)^* + SO_4^{2-} \quad (3)$$

$$(CdS)^* \rightarrow CdS + h\nu \quad (4)$$

Figure S2 illustrates that stable ECL signal-time curve could be obtained under continuous potential scanning for 25 cycles. Such results suggested that CdS NCs/GCE is a good platform for further construction of ECL sensing systems.

Previous reports have indicated that on a cytosine-rich oligonucleotide template ultra-small Ag nanoclusters could be synthesized by chemical reduction of silver ions under mild conditions.[29] In order to obtain Ag nanoclusters, a typical cytosine-rich sequence containing 12 bases was chosen as the template and the inhibitor on the growth of nanoclusters once a desired size was

reached.[18, 30] Figure 1A shows that there is an absorption band at the peak of 515 nm in the UV-vis spectrum, which could be assigned as the characteristic peak of ultra-small Ag nanoclusters encapsulated with oligonucleotide.[18] The strong absorption at 415 nm could be ascribed to the plasmon resonance of larger Ag nanoparticles in aqueous solution.[31] It could be found that the surface plasma absorption of oligonucleotide encapsulated Ag nanoclusters showed good overlap with the ECL emission of CdS NCs film at 520 nm, which is a key element for efficient energy transfer in ECL systems.[4,32] Therefore, such Ag nanoclusters may be utilized as suitable ECL energy acceptors to effectively quench ECL from CdS NCs.

To further characterize the prepared Ag nanoclusters, their morphology was investigated by TEM image. Figure 1B illustrates some large Ag nanoparticles with the average diameter of 4.05 ± 0.69 nm (Inset in Figure 1B) and a large amount of small Ag nanoclusters (highlighted in red circles), which were spherical and dispersed well in solution. The average diameter of small Ag nanoclusters was calculated to be 1.59 ± 0.23 nm, which agreed well with those in previous reports..[18, 33]

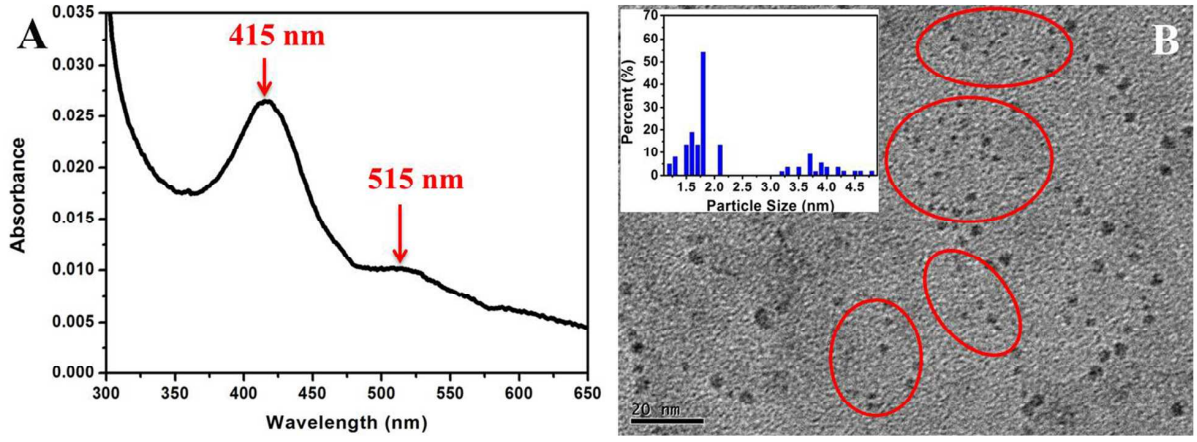

Figure 1. The UV-vis spectrum (A) and, the TEM image (B) of Ag nanoclusters and the size distribution of Ag NPs and Ag nanoclusters (B Inset).

Sensing Principle and Characterization of the ECL Sensor

Scheme 1 illustrates the application of oligonucleotide encapsulated Ag nanoclusters as both electro-catalyst for $K_2S_2O_8$ reduction and ECL energy acceptor of CdS NCs for MiRNA sensing. A molecular beacon (MB) with a thiol group at its 5' end was immobilized on a CdS NCs film modified glass carbon electrode (CdS NCs/GCE), followed by adding 6-Mercapto-1-hexanol (MCH) to block active sites. After hybridized with the target MiRNA and oligonucleotide encapsulated Ag nanoclusters, the hairpin structure opened up and then Ag nanoclusters would be in close proximity to CdS NCs on the modified glass carbon electrode.

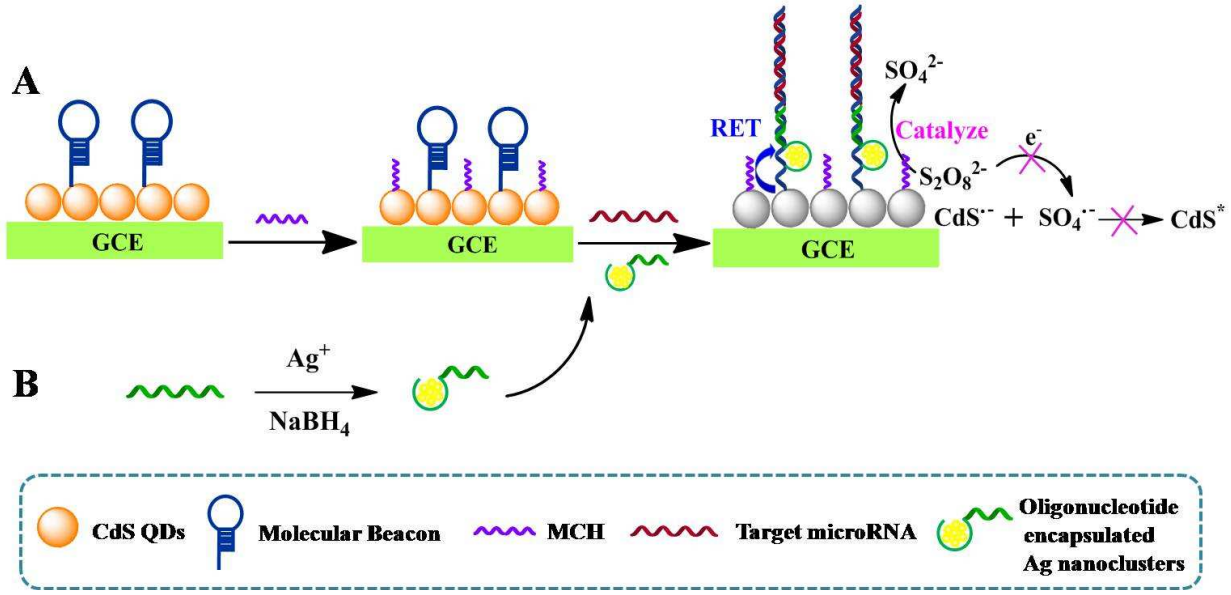

Scheme 1. Quenched ECL for detection of miRNA using oligonucleotide encapsulated Ag nanoclusters based on ECL RET and electron transfer (A) and the synthesis of oligonucleotide encapsulated Ag nanoclusters (B).

ECL signals (Figure 2A) and electrochemical impedance spectroscopy (Figure S3) were applied to characterize the fabrication process of the ECL sensing system. As shown in Figure 2, it could be found that ECL intensity decreased a little bit after the immobilization of hairpin probe and MCH on the CdS NCs modified GCE (Figure 2A, curves b and c) compared with that of CdS NCs film before assembly (Figure 2A, curve a). Upon hybridization of 1.0 nM target miRNA and 0.2 μM oligonucleotide encapsulated Ag nanoclusters, the quenching efficiency of 88.2% for ECL intensity was obtained (Figure 2A, curve d) because of the unfolding process of the DNA hairpin. Figure 2B shows the influence of hybridization with target miRNA and oligonucleotide encapsulated Ag nanoclusters on the ECL spectra of MCH/MB/CdS NCs/GCE. It could be observed that the ECL quenching efficiency at 520 nm was much larger than that at other wavelengths, indicating that an effective ECL RET between CdS NCs and Ag nanoclusters occurred, which agreed well with the good spectral overlap between the ECL emission spectrum of CdS NCs film and the absorption bands of Ag nanoclusters as well as the very short ECL energy donor-acceptor separation distance.

There are two possible interferences that need to be discussed. During the synthesis process, some Ag nanoparticles would be produced accompanied with Ag nanoclusters in solution.

However they could not be encapsulated by oligonucleotide sequence because of their sizes. Thus, after hybridization they could be rinsed away without influences on the ECL sensing system. On the other hand, the Ag nanoclusters combined with functional oligonucleotide sequence CCC TAA CTC CCC was reported to emit photoluminescence signal at the wavelength of ~700 nm.[34] Such wavelength is out of the limitations of the instruments and could not affect the ECL spectra in the range of wavelength from 420 to 660 nm. Our experimental results shows that no obvious enhancement emission could be found at longer wavelengths, suggesting that during ECL RET process no emission of Ag nanoclusters was produced and ECL excitation energy of CdS NCs was effectively dissipated in Ag nanoclusters.

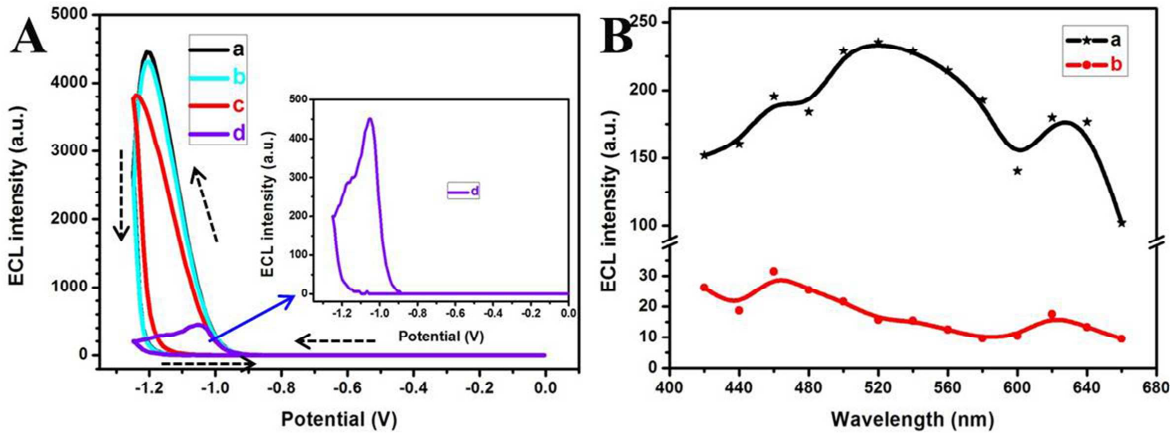

Figure 2. (A) Cyclic ECL intensity on potential curves of CdS NCs/GCE (a), MB/CdS NCs/GCE (b), MCH/MB/CdS NCs/GCE (c) and MCH/MB/CdS NCs/GCE (d) after hybridization with 1.0 nM target miRNA and 0.2 μM oligonucleotide encapsulated Ag nanoclusters. Scan direction was indicated by black dashed arrows. Inset in (A): amplified plot (d). (B) The ECL spectra of MCH/MB/CdS NCs/GCE before (a) and after (b) hybridization with

1.0 nM target miRNA and 0.2 μM oligonucleotide encapsulated Ag nanoclusters obtained through filters under a cyclic potential scan from 0 to -1.25 V. The buffer: 0.1 M PBS buffer (pH 8.3) containing 0.05 M $K_2S_2O_8$.

Figure 3A shows corresponding cyclic voltammograms (CVs) in ECL detecting process, indicating that after hybridization the peak current could be enhanced by 35.6% and the reduction potential shifted positively from -1.20 V to -1.10 V. Moreover, a new ECL peak appeared at -1.04 V (the Inset of Figure 2A). Such results could be attributed to the fact that Ag nanoclusters in situ synthesized on oligonucleotide possessed exceptional metal mimic enzyme properties.[18] Thus, after hybridization the oligonucleotide encapsulated Ag nanoclusters not only acted as a conductive material for effectively reducing the injection barrier of electrons in ECL reaction but also electro-catalytically reduced coreactant $K_2S_2O_8$ to the product SO_4^{2-}. As a result, the reduction peak current of $K_2S_2O_8$ was significantly enhanced, leading to the generation of a new ECL peak at a relatively positive potential. On the other hand, the coreactant of ECL was consumed near the electrode surface, giving rise to a substantial decrease of ECL intensity and contributing together to the total quenched ECL intensity in ECL RET.

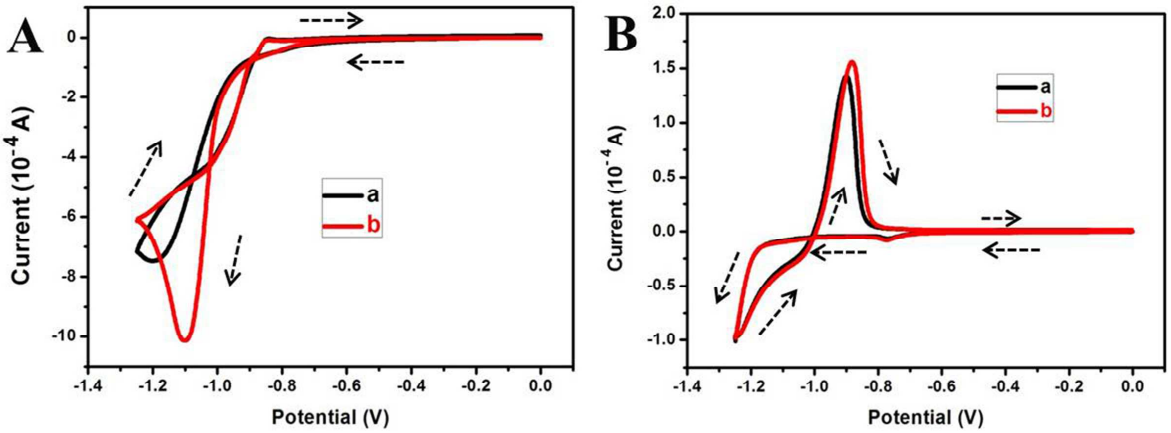

Figure 3. (A) CVs of the MCH/MB/CdS NCs/GCEs before (a) and after (b) hybridization with 1.0 nM target miRNA and 0.2 μM oligonucleotide encapsulated Ag nanoclusters. Buffer: 0.1 M PBS buffer (pH 8.3) containing 0.05 M $K_2S_2O_8$. (B) CVs of the MCH/MB/CdS NCs/GCEs before (a) and after (b) being incubated in buffer solution containing oligonucleotide encapsulated Ag nanoclusters and miRNA in deaerated 0.1 M PBS buffer (pH 8.3, bubbling N_2 for 20 min). Scan direction was indicated by black dashed arrows.

Figure 3B shows the influence of hybridization with miRNA and oligonucleotide encapsulated Ag nanoclusters on the electrochemical behaviors of CdS NCs film in deaerated 0.1 M PBS buffer. No obvious changes could be observed, indicating that Ag nanoclusters had no notable ability in catalyzing CdS NCs reduction.

The technique of EPR was utilized to quantify the anion sulfate radical $SO_4^{\bullet-}$ in the $K_2S_2O_8$ evolved ECL process after hybridization reaction. As shown in Figure 4, the hyperfine splitting constants of DMPO radical adducts (obtained by simulation, a_N = 13.64 G, a_H = 9.21 G, a_H = 1.25 G, and a_H = 0.79 G) were consistent with data reported before,[35] which were characteristic

of DMPO-$SO_4^{\bullet-}$ adducts, verifying the existence of anion sulphate radicals in the system. Meanwhile, four sharp hyperfine split peaks emerged with an intensity ratio of 1:2:2:1 and the hyperfine splitting constants were a_N = 14.68 G, a_H = 15.26 G, which were representative values of DMPO-$OH^{\bullet}$ adducts,[35-36] suggesting that $OH^{\bullet}$ also presented in the $K_2S_2O_8$ system. Hydroxyl radical may be produced in the reaction between anion sulphate radical and water, which could also react with $(CdS)^{\bullet-}$ to the excited state $(CdS)^*$ and then generate ECL signals. The processes could be expressed as follows:[37]

$$SO_4^{\bullet-} + H_2O \rightarrow HSO_4^- + OH^{\bullet} \quad (5)$$

$$(CdS)^{\bullet-} + OH^{\bullet} \rightarrow (CdS)^* + OH^- \quad (6)$$

After hybridization with target MiRNA and oligonucleotide encapsulated Ag nanoclusters, the intensities of both DMPO-$SO_4^{\bullet-}$ and DMPO-$OH^{\bullet}$ in the $K_2S_2O_8$ evolved ECL system decreased, demonstrating that less radicals of $SO_4^{\bullet-}$ and $OH^{\bullet}$ were generated. These results supported the conclusion that Ag nanoclusters near the electrode catalyzed the electrochemical reduction of $K_2S_2O_8$ to SO_4^{2-}, leading to the decrease of intermediate radials and ECL intensity.

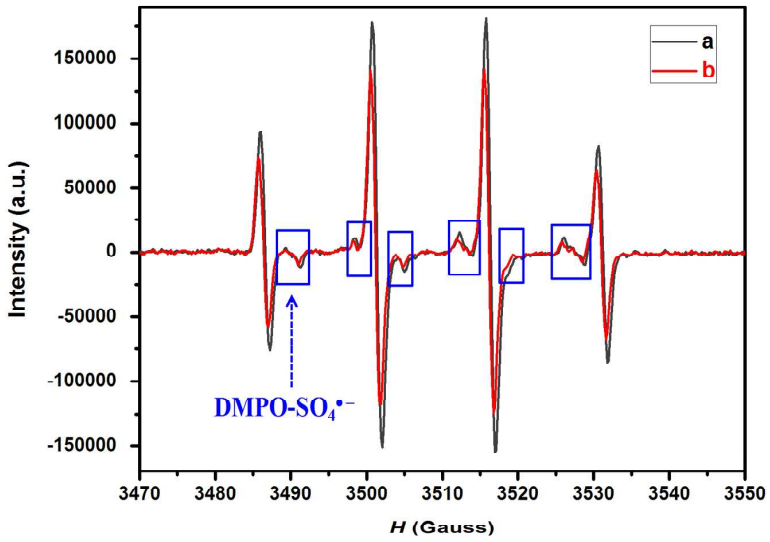

Figure 4. EPR spectra of 0.1 M PBS buffer (pH 8.3) containing 100 mM DMPO and 0.05 M $K_2S_2O_8$ after applying the potential of -1.25 V for 300 s on the MCH/MB/CdS NCs/GCE before (a) and after (b) hybridization with target miRNA and oligonucleotide encapsulated Ag nanoclusters.

Selectivity and Specificity of the Proposed MiRNA Sensing System

In the following, our approach was applied for sensitive detection of miRNA based on the synergistic effect of RET and electron transfer by using oligonucleotide encapsulated Ag nanoclusters as labels. Figure S4 shows the influence of the incubation time of miRNA and oligonucleotide encapsulated Ag nanoclusters on the ECL intensity. It could be found that the efficiency of ECL quenching increased with the increase of the incubation time from 0 to 90 min, and reached a platform after 60 min. Thus, 60 min was selected for following experiments.

The sensitivity of the system on detection of miRNA was studied with the concentrations of both MB and oligonucleotide encapsulated Ag nanoclusters at 0.2 μM. It could be observed from Figure 5A that after incubated in PBS buffer containing 0.2 μM oligonucleotide encapsulated Ag nanoclusters, the ECL emission decreased 52.6%, which was much smaller than that caused by target miRNA. As shown in Figure S5, the specific response of MB to target miRNA was demonstrated using gel electrophoresis. Therefore, miRNA could be quantified using quenched ECL signals with our approach. Based on the ECL signals (Inset in Figure 5A), the integrated ECL intensity could be calculated to be logarithmically related to the concentration of target miRNA in the range from 10 fM to 100 pM (R=96.5%, shown in Figure 5B). The regression equation could be expressed as $y = -432.2x - 3296$ (y represents the integrated ECL intensity; x represents the logarithmical concentration of miRNA). Our results were comparable to other sensing methods reported in previous literatures[9, 18, 38, 39].

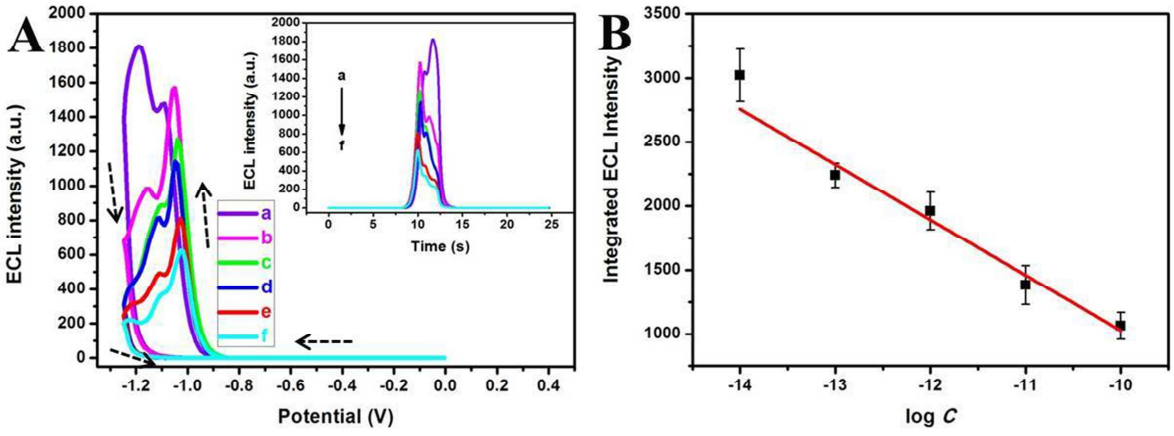

Figure 5. Cyclic ECL signal curves (A) and the calibrated ECL-concentration curve (B) for the target miRNA with different concentrations with the miRNA Sensing System. Inset in (A):

corresponding ECL signals via time. The concentrations of the target miRNA: (a) 0, (b) 10 fM, (c) 100 fM, (d) 1 pM, (e) 10 pM, (f) 100 pM. Three measurements were tested for each point. Scan direction was indicated by black dashed arrows.

The selectivity of the Ag nanoclusters-based miRNA ECL biosensor was studied by measuring the ECL responses to three types of miRNA including complete complementary target miRNA sequence, the one base mismatched MiRNA sequence or the three bases mismatched miRNA sequence, respectively. As shown in Figure 6, in the presence of complementary target miRNA sequence (a), the integrated ECL intensity was much bigger than that of single base (b) or three bases (c) mismatched sequences. Such results indicated that the developed sensing system could selectively differentiate MiRNA with sequence specificity. Therefore, we believe that the sensing protocol we proposed has promising potential in practical application and we will pay much attention to it in our following works.

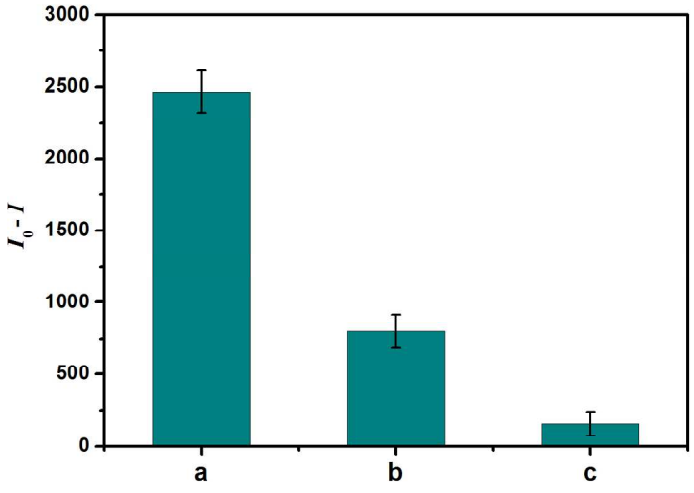

Figure 6. The integrated ECL intensity ($I_0 - I$) of MCH/MB/CdS QDs/GCE after incubated with miRNAs with complementary sequence (target miRNA) (a), single base mismatched sequence

(b), three bases mismatched sequence (c), respectively, in buffer solution containing oligonucleotide encapsulated Ag nanoclusters. I_0 means that there were no miRNAs in solution while I means that there were miRNA in solution. I_0 and I were Different Three measurements were tested for each point.

CONCLUSIONS

Here, we used a functional oligonucleotide composed of template sequence for in situ synthesis of Ag nanoclusters and their application for sensitive determination of miRNA based on quenched ECL from CdS NCs. On the one hand, effective ECL RET between CdS NCs and Ag nanoclusters could be obtained with decreased ECL because of the well spectral overlap between ECL spectrum of CdS NCs and absorption band of Ag nanoclusters. On the other hand, Ag nanoclusters could consume the coreactant ($K_2S_2O_8$) in cathodic ECL process so as to decrease the ECL intensity. As a result, a sensitive quenched ECL sensing of miRNA could be achieved with a wide linear range and acceptable selectivity. We believe that this study could broaden the perspective of ECL for further development of biosensors.

ASSOCIATED CONTENT

Supporting Information

Additional characterization figures and related results discussions. This material is available free of charge via the Internet at http:// pubs.acs.org.

AUTHOR INFORMATION

Corresponding Author

*E-mail: xujj@nju.edu.cn (J.J. Xu)

Author Contributions

1: these authors contributed equally.

Notes

The authors declare no competing financial interest.

ACKNOWLEDGEMENT

We appreciate the financial support of this project from National Natural Science Foundation of China (No. 21535003, 21475058, 21135003). This work was also supported by a Project Funded by the Priority Academic Program Development of Jiangsu Higher Education Institutions.

REFERENCES

1. Richter, M. M. Electrochemiluminescence (ECL). *Chem. Rev.* **2004**, *104* (6), 3003-3036.

2. Miao, W. Electrogenerated Chemiluminescence and Its Biorelated Applications. *Chem. Rev.* **2008**, *108* (7), 2506-2553.

3. Wu, P.; Hou, X.; Xu, J.-J.; Chen, H.-Y. Electrochemically Generated versus Photoexcited Luminescence from Semiconductor Nanomaterials: Bridging the Valley between Two Worlds. *Chem. Rev.* **2014**, *114* (21), 11027-11059.

4. Shan, Y.; Xu, J.-J.; Chen, H.-Y. Distance-Dependent Quenching and Enhancing of Electrochemiluminescence from a CdS:Mn Nanocrystal Film by Au Nanoparticles for Highly Sensitive Detection of DNA. *Chem. Commun.* **2009**, (8), 905-907.

5. Shan, Y.; Xu, J.-J.; Chen, H.-Y. Electrochemiluminescence Quenching by CdTe Quantum Dots Through Energy Scavenging for Ultrasensitive Detection of Antigen. *Chem. Commun.* **2010**, *46* (28), 5079-5081.

6. Wu, M.-S.; Shi, H.-W.; Xu, J.-J.; Chen, H.-Y. CdS quantum dots/$Ru(bpy)_3^{2+}$ Electrochemiluminescence Resonance Energy Transfer System for Sensitive Sytosensing. *Chem. Commun.* **2011**, *47* (27), 7752-7754.

7. Wu, M.-S.; He, L.-J.; Xu, J.-J.; Chen, H.-Y. RuSi@$Ru(bpy)_3^{2+}$/Au@Ag_2S Nanoparticles Electrochemiluminescence Resonance Energy Transfer System for Sensitive DNA Detection. *Anal. Chem.* **2014**, *86* (9), 4559-4565.

8. Liu, J.; He, X.; Wang, K.; He, D.; Wang, Y.; Mao, Y.; Shi, H.; Wen, L. A Highly Sensitive Electrochemiluminescence Assay for Protein Kinase based on Double-quenching of Graphene Quantum Dots by G-quadruplex–hemin and Gold Nanoparticles. *Biosens. Bioelectron.* **2015**, *70*, 54-60.

9. Cheng, Y.; Lei, J.; Chen, Y.; Ju, H. Highly Selective Detection of MicroRNA based on Distance-dependent Electrochemiluminescence Resonance Energy Transfer between CdTe Nanocrystals and Au Nanoclusters. *Biosens. Bioelectron.* **2014**, *51*, 431-436.

10. Shan, Y.; Xu, J.-J.; Chen, H.-Y. Distance-Dependent Quenching and Enhancing of Electrochemiluminescence from a CdS: Mn Nanocrystal Film by Au Nanoparticles for Highly Sensitive Detection of DNA. *Chem. Commun.* **2009**, (8), 905-907.

11. He, L.-J.; Wu, M.-S.; Xu, J.-J.; Chen, H.-Y. A Reusable Potassium Ion Biosensor Based on Electrochemiluminescence Resonance Energy Transfer. *Chem. Commun.* **2013**, *49* (15), 1539-1541.

12. Niu, H.; Yuan, R.; Chai, Y.; Mao, L.; Liu, H.; Cao, Y. Highly Amplified Electrochemiluminescence of Peroxydisulfate Using Bienzyme Functionalized Palladium Nanoparticles as Labels for Ultrasensitive Immunoassay. *Biosens. Bioelectron.* **2013**, *39* (1), 296-299.

13. Zhou, H.; Zhang, Y.-Y.; Liu, J.; Xu, J.-J.; Chen, H.-Y. Efficient Quenching of Electrochemiluminescence from K-Doped Graphene-CdS:Eu NCs by G-Guadruplex-Hemin and Target Recycling-Assisted Amplification for Ultrasensitive DNA Biosensing. *Chem. Commun.* **2013**, *49* (22), 2246-2248.

14. Jie, G.-F.; Liu, P.; Zhang, S.-S. Highly Enhanced Electrochemiluminescence of Novel Gold/Silica/CdSe-CdS Nanostructures for Ultrasensitive Immunoassay of Protein Tumor Marker. *Chem. Commun.* **2010**, *46* (8), 1323-1325.

15. Wu, L.; Wang, J.; Ren, J.; Li, W.; Qu, X. Highly Sensitive Electrochemiluminescent Cytosensing Using Carbon Nanodot@Ag Hybrid Material and Graphene for Dual Signal Amplification. *Chem. Commun.* **2013**, *49* (50), 5675-5677.

16. Wang, X.-F.; Zhou, Y.; Xu, J.-J.; Chen, H.-Y. Signal-On Electrochemiluminescence Biosensors Based on CdS-Carbon Nanotube Nanocomposite for the Sensitive Detection of Choline and Acetylcholine. *Adv. Funct. Mater.* **2009**, *19* (9), 1444-1450.

17. Wang, J.; Zhao, W.-W.; Zhou, H.; Xu, J.-J.; Chen, H.-Y. Amplified Electrochemiluminescence Detection of DNA-Binding Protein Based on the Synergy Effect of Electron and Energy Transfer between CdS Nanocrystals and Gold Nanoparticles. *Biosens. Bioelectron.* **2013**, *41*, 615-620.

18. Dong, H.; Jin, S.; Ju, H.; Hao, K.; Xu, L.-P.; Lu, H.; Zhang, X. Trace and Label-Free MicroRNA Detection Using Oligonucleotide Encapsulated Silver Nanoclusters as Probes. *Anal. Chem.* **2012**, *84* (20), 8670-8674.

19. Wilcoxon, J. P.; Abrams, B. L. Synthesis, Structure and Properties of Metal Nanoclusters. *Chem. Soc. Rev.* **2006**, *35* (11), 1162-1194.

20. Ramnani, P.; Gao, Y.; Ozsoz, M.; Mulchandani, A. Electronic Detection of MicroRNA at Attomolar Level with High Specificity. *Anal. Chem.* **2013**, *85* (17), 8061-8064.

21. Chen, C.-Z.; Li, L.; Lodish, H. F.; Bartel, D. P. MicroRNAs Modulate Hematopoietic Lineage Differentiation. *Science* **2004**, *303* (5654), 83-86.

22. Arenz, C. MicroRNAs-Future Drug Targets? *Angew. Chem. Int. Ed.* **2006**, *45* (31), 5048-5050.

23. Hao, N.; Li, X.-L.; Zhang, H.-R.; Xu, J.-J.; Chen, H.-Y. A Highly Sensitive Ratiometric Electrochemiluminescent Biosensor for MicroRNA Detection Based on Cyclic Enzyme Amplification and Resonance Energy Transfer. *Chem. Commun.* **2014**, *50* (94), 14828-14830.

24. Duan, R.; Zuo, X.; Wang, S.; Quan, X.; Chen, D.; Chen, Z.; Jiang, L.; Fan, C.; Xia, F., Lab in a Tube: Ultrasensitive Detection of MicroRNAs at the Single-Cell Level and in Breast Cancer Patients Using Quadratic Isothermal Amplification. *J. Am. Chem. Soc.* **2013**, *135* (12), 4604-4607.

25. Liao, Y.; Huang, R.; Ma, Z.; Wu, Y.; Zhou, X.; Xing, D., Target-Triggered Enzyme-Free Amplification Strategy for Sensitive Detection of MicroRNA in Tumor Cells and Tissues. *Anal. Chem.* **2014**, *86* (9), 4596-4604.

26. Wu, C.; Cansiz, S.; Zhang, L.; Teng, I. T.; Qiu, L.; Li, J.; Liu, Y.; Zhou, C.; Hu, R.; Zhang, T.; Cui, C.; Cui, L.; Tan, W., A Nonenzymatic Hairpin DNA Cascade Reaction Provides High Signal Gain of mRNA Imaging inside Live Cells. *J. Am. Chem. Soc.* **2015**, *137* (15), 4900-4903.

27. Yu, W. W.; Qu, L.; Guo, W.; Peng, X. Experimental Determination of the Extinction Coefficient of CdTe, CdSe, and CdS Nanocrystals. *Chem. Mater.* **2003**, *15* (14), 2854-2860.

28. Jie, G.; Liu, B.; Pan, H.; Zhu, J.-J.; Chen, H.-Y. CdS Nanocrystal-Based Electrochemiluminescence Biosensor for the Detection of Low-Density Lipoprotein by Increasing Sensitivity with Gold Nanoparticle Amplification. *Anal.Chem.* **2007**, *79* (15), 5574-5581.

29. Ritchie, C. M.; Johnsen, K. R.; Kiser, J. R.; Antoku, Y.; Dickson, R. M.; Petty, J. T. Ag Nanocluster Formation Using a Cytosine Oligonucleotide Template. *J. Phys. Chem. C* **2007**, *111* (1), 175-181.

30. Yeh, H.-C.; Sharma, J.; Han, J. J.; Martinez, J. S.; Werner, J. H. A DNA−Silver Nanocluster Probe That Fluoresces upon Hybridization. *Nano Lett.* **2010**, *10* (8), 3106-3110.

31. Zhang, L.; Zhu, J.; Zhou, Z.; Guo, S.; Li, J.; Dong, S.; Wang, E. A New Approach to Light up DNA/Ag Manocluster-Based Beacons for Bioanalysis. *Chem. Sci.* **2013**, *4* (10), 4004-4010.

32. Zhou, H.; Zhang, Y.-Y.; Liu, J.; Xu, J.-J.; Chen, H.-Y. Electrochemiluminescence Resonance Energy Transfer Between CdS:Eu Nancrystals and Au Nanorods for Sensitive DNA Detection. *J. Phys. Chem. C* **2012**, *116* (33), 17773-17780.

33. Xiao, Y.; Wu, Z.; Wong, K.-Y.; Liu, Z. Hairpin DNA Probes Based on Target-Induced in situ Generation of Luminescent Silver Nanoclusters. *Chem. Commun.* **2014**, *50* (37), 4849-4852.

34. Richards, C. I.; Choi, S.; Hsiang, J.-C.; Antoku, Y.; Vosch, T.; Bongiorno, A.; Tzeng, Y.-L.; Dickson, R. M., Oligonucleotide-Stabilized Ag Nanocluster Fluorophores. *J. Am. Chem. Soc.* **2008**, *130* (15), 5038-5039.

35. Fang, G.-D.; Dionysiou, D. D.; Al-Abed, S. R.; Zhou, D.-M. Superoxide Radical Driving the Activation of Persulfate by Magnetite Nanoparticles: Implications for the Degradation of PCBs. *Appl. Catal., B* **2013**, *129*, 325-332.

36. Deng, S.; Hou, Z.; Lei, J.; Lin, D.; Hu, Z.; Yan, F.; Ju, H. Signal Amplification by Adsorption-Induced Catalytic Reduction of Dissolved Oxygen on Nitrogen-Doped Carbon Nanotubes for Electrochemiluminescent Immunoassay. *Chem. Commun.* **2011**, *47* (44), 12107-12109.

37. Bartlett, P. D.; Cotman, J. D. The Kinetics of the Decomposition of Potassium Persulfate in Aqueous Solutions of Methanol. *J. Am. Chem. Soc.* **1949**, *71* (4), 1419-1422.

38. Zhang, P.; Zhuo, Y.; Chang, Y.; Yuan, R.; Chai, Y. Electrochemiluminescent Graphene Quantum Dots as a Sensing Platform: A Dual Amplification for MicroRNA Assay. *Anal. Chem.* **2015**, *87*, 10385-10391.

39. Neely, L. A.; Patel, S.; Garver, J.; Gallo, M.; Hackett, M.; McLaughlin, S.; Nadel, M.; Harris, J.; Gullans, S.; Rooke, J. A Single-molecule Method for the Quantitation of MicroRNA Gene Expression. *Nat. Meth.* **2006**, *3*(1), 41-46.

SYNOPSIS (Table of contents graphic)